ues of D_i/D_j (see Table IV).

If one now considers the case of He^3 and He^4 diffusion, Eq. (12) can be solved for $Q_3 - Q_4$ (the subscripts $i = 3$ for He^3 and $j = 4$ for He^4 are used) to yield

$$Q_3 - Q_4 = 2RT\left(1 - \frac{D_3/D_4}{1.155}\right). \quad (14)$$

Thus, unless $D_3/D_4 = 1.155$ at all temperatures (which has been shown experimentally not to be the case), there must be a difference in the activation energy for the diffusion of these two helium isotopes. In addition, unless the variations in D_3/D_4 with temperature exactly offset the $2RT$ term, the value of $Q_3 - Q_4$ will be temperature dependent and an Arrhenius plot of $\ln (D_3/D_4)$ vs $1/T$ will be curved. Similarly, Eq. (13) can be solved for D_{03}/D_{04} to yield

$$D_{03}/D_{04} = 2(1.155) - D_3/D_4 , \quad (15)$$

which shows that D_{03}/D_{04} also varies as a function of D_3/D_4 (which, of course, it must if $Q_3 - Q_4$ varies). Unfortunately, the scatter in the data of the present study, coupled with the small variations expected in $Q_3 - Q_4$ and D_{03}/D_{04}, prevents such a detailed analysis of the results. However, the data have been analyzed by a linear least-mean-squares technique, which effectively averages the slope and intercept values. Thus, the experimental values for $Q(He^3) - Q(He^4)$ and $D_0(He^3)/D_0(He^4)$ as shown in Eqs. (4) and (5) can be compared with the mean values of $Q_3 - Q_4$ and D_{03}/D_{04} as calculated from Eqs. (14) and (15), respectively. These values are given in Table V. In view of the various approximations made and the accuracy of the experimental data, there appears to be excellent agreement between the theoretical and experimental values. These results strongly support the validity of the quantum corrections proposed by LeClaire.

*This work was supported by the U.S. Atomic Energy Commission under Contract No. AT-(29-1)-789.

[1]D. E. Swets, R. W. Lee, and R. C. Frank, J. Chem. Phys. 34, 17 (1961).

[2]R. M. Barrer, *Diffusion In and Through Solids* (Cambridge U. P., New York, 1941), p. 117.

[3]K. P. Srivastava and G. J. Roberts, Phys. Chem. Glasses 11, 21 (1970).

[4]V. O. Altermose, J. Appl. Phys. 32, 1309 (1961).

[5]J. E. Shelby, J. Am. Ceram. Soc. 54, 125 (1971).

[6]W. M. Jones, J. Am. Chem. Soc. 75, 3093 (1953).

[7]J. R. Manning, *Diffusion Kinetics for Atoms in Crystals* (Van Nostrand, Princeton, N. J., 1968), p. 127.

[8]A. D. LeClaire, Phil. Mag. 14, 1271 (1966).

[9]R. C. Frank, D. E. Swets, and R. W. Lee, J. Chem. Phys. 35, 1451 (1961).

[10]J. G. Mullen, Phys. Rev. 121, 1649 (1961).

PHYSICAL REVIEW B VOLUME 4, NUMBER 8 15 OCTOBER 1971

Calculation of the Optical Properties of Amorphous SiO_x Materials

Alan J. Bennett and L. M. Roth
General Electric Corporate Research and Development, Schenectady, New York 12301
(Received 4 June 1971)

The electronic structure and optical behavior of materials of the amorphous series SiO_x with $0 \leq x \leq 2$ are calculated using a quantum chemical cluster approach. These materials are both compositionally and structurally disordered, and exhibit energy gaps ranging from ~1 eV for Si to ~9 eV for SiO_2. Each composition, i.e., value of x, is represented here by a number of topologically distinct clusters each containing 8 silicon atoms and $8x$ oxygen atoms. Each silicon is tetrahedrally coordinated with y oxygens and $4-y$ silicons with $0 \leq y \leq 4$ and $\langle y \rangle = 2x$. We saturate peripheral bonds by a generalization of the periodic boundary conditions appropriate for a regular array. A simple molecular-orbital scheme, the extended Hückel theory, is applied to obtain electronic energy levels for each cluster. Using the indirect constant-matrix-element approximation and taking a weighted average over the various configurations, we obtain the imaginary part of the dielectric constant for a given composition x. The calculated results are in rather good semiquantitative agreement with the experimental results of Philipp, including the variation of the energy gap with composition and the general shape of the ϵ_2-vs-frequency curves.

I. INTRODUCTION

Silicon and oxygen may be combined to form amorphous materials of composition SiO_x with x varying from 0 to 2. The optical properties of amorphous Si,[1] SiO,[2] $SiO_{1.5}$,[2] and SiO_2[3] have been studied by many investigators. Recently, Philipp[4] reported systematic measurements of the absorption coefficient and reflectance of SiO, $SiO_{x\sim1.5}$, and SiO_2. These materials exhibit a wide spectrum of

band gaps ranging from ~1 for amorphous silicon to ~9 eV for amorphous silicon dioxide. This characteristic is, in part, responsible for their use in multilayer filters for modifying the reflectance of dielectrics and metals.

X-ray diffraction measurements[5] have indicated that silicon exhibits tetrahedral coordination in the amorphous state, and that amorphous[6] SiO_2 consists of a random network of Si atoms tetrahedrally coordinated with oxygen atoms, each of which links two Si atoms. For intermediate compositions, e.g., SiO, there is some difference of opinion as to the interpretation of the various x-ray results.[6,7] The samples used may possibly not have the same structure. Some investigators[7] have held SiO to be a mixture of SiO_2 and Si, i.e., a two-phase system. The x-ray results can also[8] be interpreted on the basis of a random network model in which each silicon is tetrahedrally coordinated with y silicons and $4-y$ oxygens, with y ranging from 0 to 4. Each oxygen connects two silicons. This model was used by Philipp[4] in interpreting his optical results which were not in accord with a two-phase model. Philipp concluded that the optical phenomena could be qualitatively accounted for by the presence of groupings of Si—O and Si—Si bonds. In particular, the statistically determined relative number of Si-(O_4) and Si-(Si_4) tetrahedra in each alloy was correlated with its optical properties.

In recent years, a variety of calculations of the electronic properties of random alloys have been performed. Most are based on the single-site approximation in which the true medium surrounding a given atom is represented by an effective one.[9] The simplest such approach, the virtual crystal approximation in which all the atoms of the material are represented by the same average properties, have been used to study the $GeSi_x$ system.[10] Velicky, Kirkpatrick, and Ehrenreich[9] have noted, however, that the approach may not predict physically present band gaps. The average matrix approximation introduced by Beeby and Edwards[11] has been shown,[9,12] on the other hand, to introduce spurious band gaps. The coherent potential approximation, due to Soven,[12,13] is a considerable improvement on the previous approximations. It has so far been applied only to very simple models and it is not immediately clear how it can be applied to the present system.

Gubanov[14] has described a second general approach to the calculation of alloy properties. A selected cluster of atoms is prescribed, with an average being taken over all the atoms external to that cluster. A second average is then taken over the configuration of the selected group of atoms. This technique is justified by the observation that electronic properties of amorphous semiconductors and insulators are determined by their short-range order.[15–17] Abarenkov *et al.*,[18] have used a somewhat similar approach to calculate the energy gap in SiO_2 and GeO_2. The cluster used contained one silicon (germanium) atom and four oxygen atoms with only certain directed orbitals on each oxygen being included in the calculation.

This paper presents a calculation based on this second general approach. We apply quantum chemical methods to a cluster of Si and O atoms arranged in a network as in Philipp's analysis. This quantum chemical cluster approach has been used previously in studies of chemisorption,[19,20] and of defects in SiO_2[21] and diamond.[22] For a material of composition SiO_x, we include in our cluster 8 Si and $8x$ O atoms. We consider a variety of configurations and then average the final results for optical properties over the configurations. Since cohesive energies of the configurations are not calculated with sufficient reliability, no Boltzmann factors are used in the averaging. The various configurations are distinguished by the number of nearest- and next-nearest-neighbor oxygen atoms in the network. Oxygen and silicon positions for each configuration are determined from a set of rules based on the lattice parameters of crystalline silicon and β-crystobalite, the SiO_2 crystal most similar to the presumed structure of amorphous SiO_2.[21,23]

By assuming a prescribed set of fixed positions for the oxygen atoms, our calculations ignore much of the structural disorder associated with shifts of lattice constant and bond angle in an amorphous sample. Compositional disorder is emphasized. Experimental studies of amorphous vs crystalline elemental semiconductors[24] and semiconducting GeSi alloys[1] indicate that the disorder tends to smooth out the electronic density of states and reduce the band gap by tenths of an eV. These changes are much smaller than the experimentally observed differences between the optical characteristics of the different SiO_x materials.

As described below, the boundary atoms in each configuration are interconnected in order to eliminate dangling bonds. Such dangling bonds may, however, actually be present[25] in amorphous materials due to the presence of voids, etc.

The electronic energy levels associated with a given cluster are calculated using a very simple molecular-orbital approximation, the extended Hückel theory[26] popularized by Hoffman. The technique is not a self-consistent one and, as a result, only semiquantitative results may be expected for the materials with high oxygen content. Better, but more computer-time-consuming, molecular-orbital schemes[27] have been developed and could eventually be applied to the alloy problem.

The imaginary part of the interband dielectric constant ϵ_2 is calculated in the indirect constant-matrix-element approximation.[28] That is, the lack of long-range order is assumed to eliminate $\vec{k}$ con-

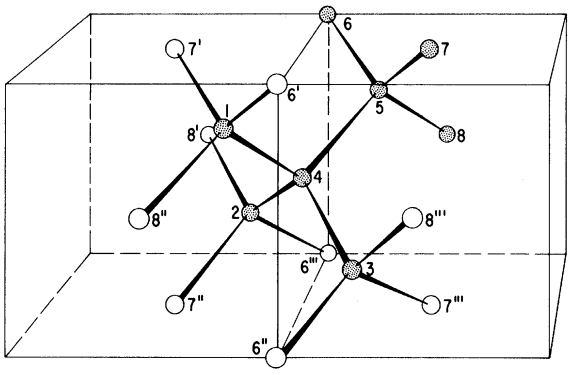

FIG. 1. Eight-atom silicon cluster (shaded circles) enmeshed in a periodic array (open circles). Primed sites (e.g., 7′) are equivalent to unprimed sites (e.g.,7).

servation, and the momentum matrix element is taken to be a constant. This assumption has been shown adequate to account for the optical properties of a variety of amorphous materials.

Section II A describes the determination of the various lattice configurations and their connectivity. The extended Hückel theory is briefly discussed in Sec. II B. Section III contains our results and a comparison with Philipp's data. Some conclusions are presented in Sec. IV.

II. METHOD

A. Lattice Configurations

We now wish to construct clusters of silicon and oxygen to represent the compounds intermediate between silicon and SiO_2. We shall work with clusters of 8 silicons and n oxygens where n ranges from 0 to 16. We begin with pure silicon for which we adopt a crystalline model, i.e., the diamond lattice with nearest neighbor distance of 2.36 Å. This ignores the density changes in going from the crystalline to amorphous phase. For this case, we use the cluster of eight silicons shown in Fig. 1, and assume it to be part of a periodic array in order to eliminate the dangling bonds at the edge of the cluster. This is indicated in Fig. 1, and we note that the appropriate unit cell for this case is that for the simple cubic lattice. In the calculation we require the wave function to be periodic over this unit cell. Thus for Fig. 1, we assume that the amplitude of an orbital on atom 7′ is equal to the amplitude of the orbital on 7, and so forth. Thus the bond connecting 7′ and 1 in the figure effectively connects 7 and 1, and this amounts to tying up the bonds around the outside of the cluster. These outside bonds correspond to additional matrix elements in the Hamiltonian matrix described below. The procedure is described in more detail in our SiO_2 paper.[21] The calculation is equivalent to a linear combination of atomic orbitals (LCAO) energy-band calculation carried out at a finite number of k values in the Brillouin zone.

The situation can be visualized more easily by using a two-dimensional model—a cluster of six atoms considered as part of a hexagonal net. This is shown in Fig. 2(a) in which we show how the cluster is repeated periodically. Figure 2(b) shows the cluster together with the outside bonds which must be saturated.

We now consider SiO_2, which is represented by a simplified version of the β-crystoballite structure. This structure can be obtained[21] from the diamond lattice of silicon by simply inserting oxygens midway between all silicon nearest-neighbor pairs, i.e., by replacing all Si–Si bonds with oxygen bridges. This includes in Fig. 1 the nine outside bonds (1—6′, 1—7′, etc.) as well as the seven bonds. In order to accommodate the oxygens we must expand the lattice so that the Si-Si distance changes from 2.36 to 3.1 Å. The two-dimensional version of this process is shown in Fig. 2(c).

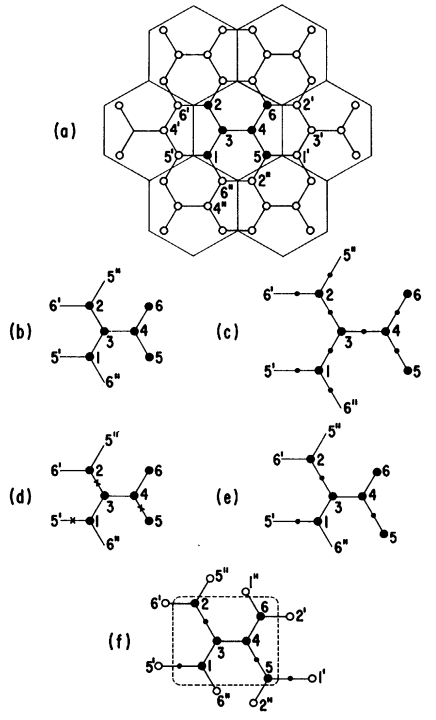

FIG. 2. Two-dimensional six-silicon illustrational cluster (large solid circles): (a) enmeshed in periodic array; (b) showing outside bonds to be saturated; (c) with oxygens (small solid circles) inserted at all possible sites; (d) with crosses marking sites for insertion of three oxygens; (e) after insertion of the three oxygens (small solid circles) and expansion of the required Si-Si separations; (f) showing the three-oxygen-atom example embedded in larger system.

For the intermediate case Si_8O_n, it seems reasonable to suppose the silicon positions to be topologically equivalent to both the limiting cases of Si and SiO_2. Thus we shall consider the silicon structure of Fig. 1, or the two-dimensional example of Figs. 2(a) and 2(b), and we now wish to replace n of the silicon bonds by oxygen bridges and to increase the corresponding Si-Si separations. There are a variety of ways to choose which bonds to change, and this will be discussed further below. Having chosen a given configuration, however, imagine first marking the bonds in the cluster to be changed as in Fig. 2(d), and then increasing the corresponding Si-Si distances without changing any directions. This is illustrated in Fig. 2(e), for our two-dimensional example. We can tie up the outside bonds in this case in the same manner as described above, even though the configuration produced for the cluster can no longer be continued periodically. The cluster is, in fact, periodic in a warped hyperspace.

To characterize this procedure more precisely for the two- or three-dimensional case, and to show how to calculate all nearest-neighbor Si-Si overlaps in this model, let us define the vector matrix $\vec{D}_{ij}$ $(i, j = 1 - 8)$ as follows. For pure silicon, if i and j are nearest-neighbor silicons in the cluster, then $\vec{D}_{ij} = \vec{R}_j - \vec{R}_i$, i.e., $\vec{D}$ defines the vector distance between them. If i and j' are nearest neighbors, i.e., if i is a neighbor of a displaced version of j in the periodic continuation, then $\vec{D}_{ij} = \vec{R}_{j'} - \vec{R}_i$: similarly for i' and j. Otherwise we take $\vec{D}_{ij}$ to be zero. We see that $\vec{D}_{ij}$ is well defined for all i and j in the cluster and furthermore that all nearest-neighbor overlaps including outside bonds as well as inside ones can be calculated using $\vec{D}_{ij}$.

Now, for Si_8O_n, suppose x_{ij} is 1 unless i and j are connected by an oxygen bridge in which case $x_{ij} = d$, where d is the ratio of the Si-Si distance in SiO_2 to that in Si. Then for Si_8O_n we define the vector matrix $\vec{D}'_{ij'} = x_{ij}\vec{D}_{ij}$. By the use of $\vec{D}'_{ij}$, we can calculate all overlaps between neighboring silicons and between these and the intervening oxygen if it is there. Thus our procedure is determinate for first neighbors. It is also determinate for second neighbors. Thus we can define a second-neighbor distance between i and k in the cluster through j. We have

$$\vec{D}'_{ijk} = \vec{D}'_{ij}\vec{D}'_{jk},$$

assuming ij and jk are neighbor pairs. This vector distance can be used to calculate overlaps between i and k. Note the dependence on j. If we are to include second-neighbor overlaps we must add up the overlaps for equivalent atoms inside and outside the cluster. Thus for atoms 1 and 4 in Fig. 2(a) we need overlaps between 1 and 4, 1 and 4′, and 1 and 4″. These are characterized by the index j, which in this case has values 3, 5, and 6. In the three-dimensional crystal each second-neighbor pair has four overlaps, one inside and three outside.

This procedure breaks down, however, if we try to go to third neighbors. For example, in Fig. 2(a) the distance between 1 and 5 via the paths 1, 3, 4, 5 and 1, 6″, 2″, 5 are the same and there is no preferred choice of the two paths. When oxygens are added in selected intermediate sites, the two paths are no longer necessarily equivalent, and so the distance is not well defined.

We should emphasize here that the relatively simple scheme we have developed works only for a sufficiently small cluster. For a larger cluster, we would certainly have to bend and twist the bonds. For our particular choice of cluster, we have a well-defined way of calculating first- and second-neighbor silicon-silicon Hamiltonian matrix elements, given a configuration of bonds and bridges. As noted below, the oxygen wave functions are contracted relative to those of silicon and so only nearest-neighbor Si-O overlaps are needed.

It is interesting to compare our scheme with one of Gubanov's[14] proposals. He equated the modulus of the wave function on an atom external to his cluster to one, and let the phase be determined by a factor $e^{i\vec{k}\cdot\vec{R}_e}$, with $\vec{k}$ an arbitrary wave vector and $\vec{R}_e$ the position vector of the external atom. He envisioned averaging over external atom positions. An analogous boundary condition for our work might be $\psi_{6'} = \psi_6 e^{i\vec{k}\cdot(\vec{R}_6 - \vec{R}_{6'})}$ etc. If we were to average the final results (density of states) over a suitable range of $\vec{k}$, such a boundary condition would lead to exact results in the crystalline case.

Consider now the choice of positions for the n oxygens of the Si_8O_n cluster. We shall assume that the oxygens are to be distributed at random among the available sites. For our finite cluster we would ideally wish to calculate the level structure for all possible configurations and perform a suitable average. Let us now explore the feasibility of this scheme.

For a given value of n there are $\binom{16}{n}$ ways of choosing n of the 16 possible bonds to be converted to bridges. However, because of the symmetry of the cluster, not all of these ways are independent. Thus for $n = 1$ all 16 possible sites for the oxygen are equivalent. For the general case we can determine how many configurations are equivalent to a given configuration C by considering the group of G symmetry operations which take our set of 16 sites into themselves. We emphasize that we are considering the cluster as periodically extended. Then clearly all 48 operations of the cubic point group will take the lattice into itself and permute the 16 sites. In addition we have the fact that our unit cell contains four primitive unit cells of the diamond

lattice, so that there are four translations. Altogether there are $4\times48=192$ space-group operations which permute the 16 sites into an equivalent set of 16.

However, if we are considering a given configuration, some of the above operations may not change the configuration at all. These form a group of order G_c. Then the number of different configurations equivalent to c is $N_c=G/G_c$. For our example of $n=1$, we see from Fig. 1 (putting the oxygen between silicons 4 and 5) that the oxygen position is unchanged if we perform the six operations of the triangle group with or without an inversion through the oxygen. We therefore have $G_c=12$, so that $N_c=192/12=16$, as we have already discovered.

The analysis of the configurations into sets of equivalent configurations rapidly becomes tedious. For $n=4$, there are 1820 configurations and for $n=8$, 12 870 configurations. To simplify the calculations, we note that configurations can also be classified by the number of first-, second-, and third-neighbor O-O pairs. Each O-O pair falls into one of these categories, as an inspection of Fig. 1 indicates. Two configurations with different neighbor distributions are surely distinct (i.e., not equivalent) although the converse is not true. The classification by neighbor distribution can be readily accomplished by computer. We then are able to make the more complete breakdown by inspection for $n=4$. We found 20 distinct configurations with weights from 6 to 192, and of these 15 accounted for 95% of the total.

It may be argued that two configurations with the same number of first-, second-, and third-neighbor O-O pairs may well have extremely similar energy spectra even though they are not precisely equivalent. One might therefore consider only choosing one of a given neighbor distribution to represent the lot. A comparison of this method with a more complete analysis showed very similar results for $n=4$ (see the Results section). We have therefore used the neighbor distribution grouping for the rest of the calculation in order to minimize computation time.

There are two possible physical interpretations which may be assigned to our model cluster. The chosen atoms may be considered to be a finite representation of the entire amorphous sample which actually contains $\sim10^{23}$ atoms. In the crystalline case, analogous calculations yield energy values and wave functions at selected points in the conventional Brillouin zone. Alternatively, the cluster may represent a much smaller microregion in the sample. This latter interpretation should, in fact, require an examination of flucutations in the number of oxygen atoms contained in the cluster when considering a given SiO_x material. We shall not, in fact, pursue this here.

B. Extended Hückel Theory

The extended Hückel theory is a semiempirical LCAO–molecular-orbital scheme, which has been used extensively in quantum chemistry. Some attempts have been made to derive[29] its formulas from the full Hartree-Fock equations. It has, at any rate, proven quite useful in semiquantitative calculations,[30] although as noted in the Introduction, its weaknesses are well known.[30]

The wave functions are taken as linear combinations of all the valence orbitals $|\lambda\rangle$ centered on the various atoms of the system, i.e.,

$$\varphi_i=\sum_\lambda C_\lambda|\lambda\rangle$$

with

$$|\lambda\rangle=e^{-Z_\lambda r}r^{n_\lambda-1}Y_{lm}(\theta,\varphi)\ ,$$

where the parameters Z_λ and n_λ are either taken from atomic data[31] or empirically determined. The Schrödinger equation, written in this nonorthogonal representation, leads to the determinent

$$|H-ES|=0\ ,$$

where

$$H_{\lambda\lambda}=-I_\lambda\ ,\quad H_{\lambda\sigma}=-\tfrac{1}{2}K(I_\lambda+I_\sigma)S_{\lambda\sigma}\ ,\quad S_{\lambda\sigma}=\langle\lambda|\sigma\rangle\ ,$$

I_λ is the valence-state ionization potential,[32,33] K is an empirically determined constant generally taken equal to 1.75,[26] and $\langle\lambda|\sigma\rangle$ is an overlap integral between atomic orbitals.

The $|\lambda\rangle$ on a silicon atom are taken to be one $3s$, three $3p$ and five $3d$ atomic orbitals with $n_{s,p,d}=3$, $I_{s,p,d}=-13.53$, -7.37, and -2.06 eV, respectively, and $Z_{s,p,d}=1.84$, 1.63, and 1.63, respectively. The d orbitals are thought to be of considerable importance in the cohesion of silicates.[34] Z_s and $Z_p=Z_d$ were determined by fitting the known band structure[35] at the Γ and X points in the Brillouin zone of crystalline silicon as well as possible while holding the other parameters at their conventional atomic values.

The $|\lambda\rangle$ on an oxygen atom are taken to be one $2s$ and three $2p$ atomic orbitals with $n_{s,p}=2$, $I_{s,p}=-32.38$, and -15.85, respectively, and $Z_{s,p}=2.27$. These are all atomic values.[33] The orbital exponents $Z_{s,p}$ are large relative to those of silicon and account for a rapid decrease of the overlaps involving oxygen orbitals with internuclear distance. This permits us to include only nearest-neighbor oxygen interactions.

We include in H and S overlaps within the cluster and also overlaps around the edge (Si-Si, Si-Si-Si, Si-O, Si-O-Si) as outlined in Sec. II A. It is interesting to attempt to justify this in terms of the interpretation of our cluster as being a part of a larger structure. In the Schrödinger equation, let σ' be outside the cluster and λ, σ inside. Then we

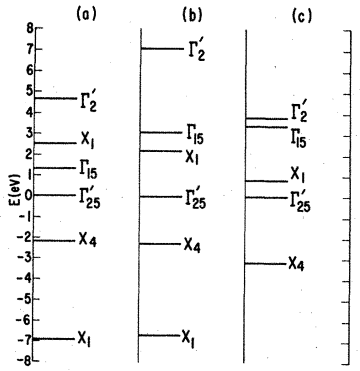

FIG. 3. Energy levels at Γ and X points of silicon Brillouin zone according to (a) present model, (b) Bassani and Yoshimine OPW calculations, and (c) Cohen-Bergstresser pseudopotential calculation.

can write

$$\sum_{\sigma} (H_{\lambda\sigma} - S_{\lambda\sigma})C_{\sigma} + \sum_{\sigma'} (H_{\lambda\sigma'} - S_{\lambda\sigma'})C_{\sigma'} = 0 \ .$$

We can truncate these equations by equating the amplitudes $C_{\sigma'}$ outside the cluster [e.g., 2′ in Fig. 2(f)] with amplitudes on selected sites inside the cluster [e.g., 2 in Fig. 2(f)]. This example adds the term $(H_{62'} - S_{62'})$ to the secular determinant in the 62 position. Similarly $(H_{26'} - S_{26'})$ is added into the 26 position. This is a way of generalizing the periodic boundary conditions. In order for the resulting matrix to be Hermitian, however, these matrix elements should be equal. This implies a rather special arrangement of the surrounding atoms as illustrated in Fig. 2(f) where the Si atom 6′ is in the same position relative to 2 as is 6 to 2′, and similarly for the other surrounding atoms. This arrangement would automatically be the case for a truly periodic structure.

III. RESULTS

The eigenenergies and eigenfunctions obtained from the calculation on the pure silicon lattice can be shown, by the application of group theory, to correspond to k states at the Γ and X points in the conventional Brillouin zone. Figure 3 shows the energy levels near the Fermi energy for those points. The corresponding results of the Bassani-Yoshimine[35] OPW and the Cohen-Bergstresser[36] pseudopotential parametrizations are shown in Figs. 3(b) and 3(c), respectively. The most serious qualitative discrepancy between our models and the others is the inversion of the X_1 and Γ_{15} levels which is responsible for the predicted direct band gap being smaller than the indirect band gap. As has been noted previously, the valence band is relatively insensitive to the parametrization used. The inaccuracy in our calculated silicon band structure could be improved with either an intensive search for parameters which allow agreement with experiment or a more sophisticated molecular-orbital scheme.[37,38] Our aim here, however, is to illustrate the general approach with the simplest possible model.

We have carried out the calculation of the electronic energy levels and wave functions for clusters with 0, 1, 2, 4, 8, 12, 14, 15, and 16 oxygens. In Figs. 4(a)-4(e) are shown histograms of the density of states for the clusters with 0, 4, 8, 12, and 16 oxygens. Table I gives some details about the actual configurations used in the calculations. The density-of-states histograms are normalized to unit volume. To accomplish this requires calculating the volumes for clusters of composition intermediate between Si and SiO_2. We have estimated these by calculating the volume for hypothetical substances with Si-Si distances scaled linearly between that for Si and SiO_2. This gives for the volume of Si_8O_x relative to Si_8

$$V = \{[(1 - \tfrac{1}{16}x)2.36 + \tfrac{1}{16}x \times 3.1]/2.36\}^3 \ .$$

In the case of Si_8 the results are extremely spikey because we have used a regular structure and only a few points in the Brillouin zone. This is less so for SiO_2, and for intermediate cases, the statistical averaging smears out such effects. In interpreting these results let us begin with SiO_2. There is a very narrow peak in the density of states in the valence band. It is primarily composed of oxygen p levels. As previously noted,[21] the present method probably overestimates the ionicity and hence the concentration of this bond on the oxygen sites.

Upon removing an oxygen and contracting the bond we have found[21] that a level appears in the energy gap. This level is occupied for electrical neutrality. It corresponds to a Si-Si bond, most simply thought of as a bonding combination of tetrahedral hybrid orbitals on adjacent silicons. As more oxygen vacancies are formed, the Si-Si bonds begin to interact, and the gap level spreads out into a band which is essentially the silicon valence band. This can be seen in Figs. 4(b)–4(d). The calculated SiO_2 conduction band is composed primarily of silicon p and d levels. When oxygen atoms are removed, this band also broadens so that the band edge moves down somewhat. The net result is an energy gap which decreases as we go toward silicon.

Looking at the system from the silicon end, the addition of oxygen results in the occurrence of an oxygen p band in the valence band of silicon, and in the opening up of the energy gap. In Fig. 5 the energy gap obtained in the present calculation is compared with gaps obtained by Philipp. We shall discuss this further below in connection with an alter-

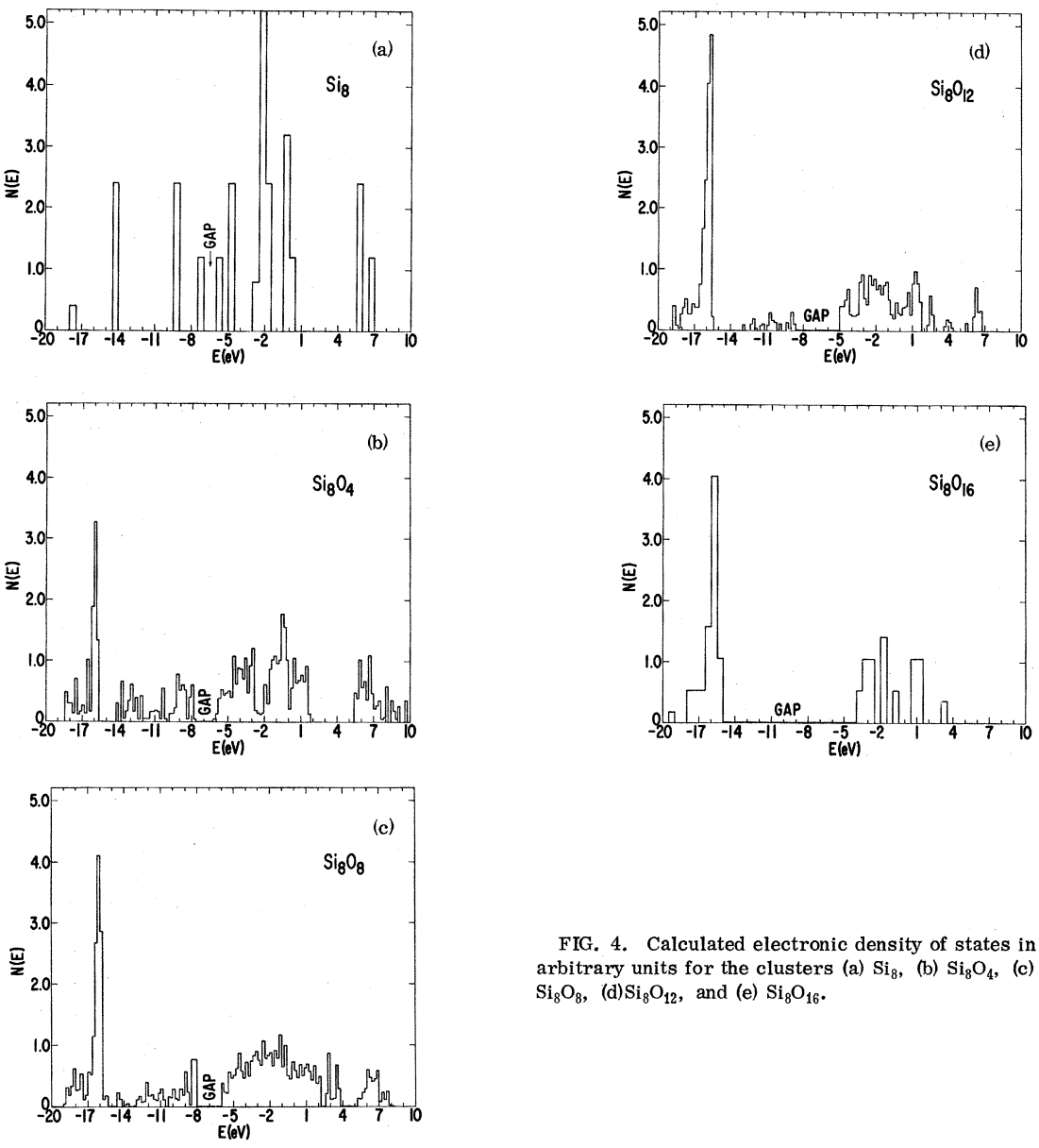

FIG. 4. Calculated electronic density of states in arbitrary units for the clusters (a) Si_8, (b) Si_8O_4, (c) Si_8O_8, (d)Si_8O_{12}, and (e) Si_8O_{16}.

native method of calculating the gap. We note here that the agreement is quite reasonable.

To compare our work more directly with the experimental results of Philipp, we calculate ϵ_2, the imaginary part of the dielectric constant. This is given for an insulator by

$$\epsilon_2(\omega) = \frac{e^2}{m^2V^2} \sum_{cv} |P_{vc}|^2 \delta(\epsilon_c - \epsilon_v - \omega) ,$$

where c and v refer to conduction and valence bands, P_{vc} is a momentum matrix element, V is the normalization volume, and the remaining symbols have their usual meanings. Recently[28] some success has been obtained for amorphous materials, by taking the momentum matrix element to be a constant and ignoring the $\vec{k}$ conservation which would occur for a regular solid. Adopting the spirit of this "indirect-constant-matrix-element" approximation, we take

$$\epsilon_2 = \frac{A}{\omega^2V^2} \left\langle \sum_{c,v} \Delta(\epsilon_c - \epsilon_v - \omega) \right\rangle_{\text{config}} .$$

Here Δ is a finite-width δ-function and A is a constant. We are thus counting the number of possible transitions within a given energy range, for a given composition, and averaging over configurations. That two factors of V are needed is clear from dimensional arguments, since the number of conduction and valence band states each increases with V.

TABLE I. Oxygen configurations used in the calculations, classified by O-O neighbor distribution. For the cases Si_8O_{12} and Si_8O_{14}, the configurations used are obtained from those for Si_8O_4 and Si_8O_2, respectively, by interchanging oxygen bridges and Si-Si bonds.

O-O neighbors 1st	2nd	No. of configs.	Configs. used[a]
		Si_8O_2	
1	0	48	14, 45
0	1	48	14, 56
0	0	24	14, 58
		Si_8O_4	
0	0	4	•••
0	4	12	•••
0	6	8	•••
1	2	96	14, 24, 38, 57
1	4	192	14, 24, 56, 38
2	1	96	28, 34, 45, 56
2	2	192	24, 34, 38, 56
2	3	384	26, 34, 45, 58
2	4	120	26, 34, 45, 57
3	2	384	36, 34, 45, 57
4	0	12	•••
4	1	192	24, 34, 45, 57
4	2	120	24, 34, 45, 58
6	0	8	•••
		Si_8O_8	
8	08	6	•••
8	12	24	•••
8	14	48	•••
8	16	12	•••
9	10	192	18, 17, 27, 28, 14, 36, 34, 56
9	12	384	17, 27, 28, 16, 34, 45, 38, 57
9	14	576	18, 28, 16, 14, 24, 36, 37, 57
10	9	192	18, 17, 27, 28, 14, 36, 34, 45
10	10	384	17, 27, 28, 14, 34, 45, 56, 37
10	11	768	18, 27, 28, 36, 34, 56, 37, 58
10	12	720	18, 27, 16, 14, 45, 56, 38, 57
10	13	1344	18, 17, 14, 24, 26, 36, 56, 58
10	14	384	17, 27, 28, 14, 24, 36, 57, 58
11	10	768	18, 27, 28, 24, 36, 34, 56, 38
11	12	1536	18, 17, 28, 24, 34, 45, 37, 57
12	8	24	•••
12	9	384	17, 27, 28, 24, 26, 34, 56, 37
12	10	720	18, 27, 28, 14, 24, 45, 37, 58
12	11	1536	18, 17, 28, 16, 36, 45, 38, 58
12	12	504	18, 28, 24, 36, 56, 38, 37, 58
13	10	1344	18, 17, 28, 16, 26, 36, 56, 57
14	8	48	•••
14	9	576	18, 28, 16, 14, 24, 26, 36, 38
14	10	384	17, 27, 28, 24, 26, 36, 37, 57
16	8	12	•••

[a]Code number shows oxygen positions in terms of neighboring silicons. Thus 14 corresponds to the oxygen between Si(1) and Si(4) as labeled in Fig. 1.

We can interpret one V as the normalization volume and the second in terms of an effective range for the averaged momentum matrix element.

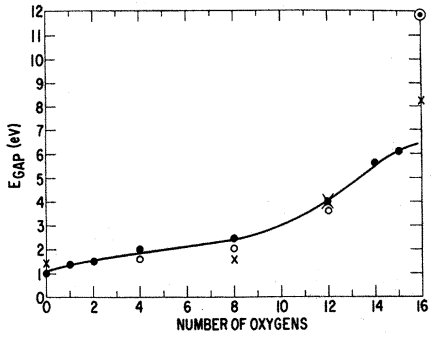

FIG. 5. Energy gap as a function of the number of oxygens: crosses, as obtained in Philipp's experiments; solid circles, as calculated from ϵ_2; open circles, as calculated from averaged electron density of states.

The results for ϵ_2 in arbitrary units are given in Figs. 6(a)–6(i) for various oxygen concentrations. Note that Figs. 6(a)–6(c) are plotted on a scale different from that used for the other curves. The histograms are the result of averaging over ensembles of configurations for each concentration as described above. For the case of four oxygens we have compared the result of averaging over all possible configurations (dashed histogram) with that of classifying configurations by oxygen neighbor distributions. Clearly there is very little difference between the curves. In particular, they resemble each other much more than they do the figures characteristic of other compositions. This justifies our use of the neighbor classification for other compositions.

Figures 6(a), 6(e), 6(f), and 6(i) can be compared with the experimental results of Philipp, which are given in Fig. 7. There is a good deal of similarity between the two sets of curves. In particular, the relative magnitudes of ϵ_2 for the four materials and many major structural features are in good qualitative agreement with experiment. For SiO_2 the theoretical histogram has peaks in it which correspond to transitions from the narrow oxygen p bond to structure in the Si p-d conduction band, and which resemble peaks in the experimental result although the rather crude approximations used here preclude making definite identifications. The persistence of this structure in the $SiO_{x\sim1.5}$ calculations as well as in the experimental results is also noteworthy. For the SiO case a double-humped structure is seen in both theory and experiment. The lower peak is due to transitions from the Si valence band to the conduction band, while the upper one is due to transitions from the oxygen p band to the conduction band. In general, it therefore appears that our relatively simple approximation is quite useful.

The results for ϵ_2 furnish us with values of the energy gap which are shown by solid circles in Fig.

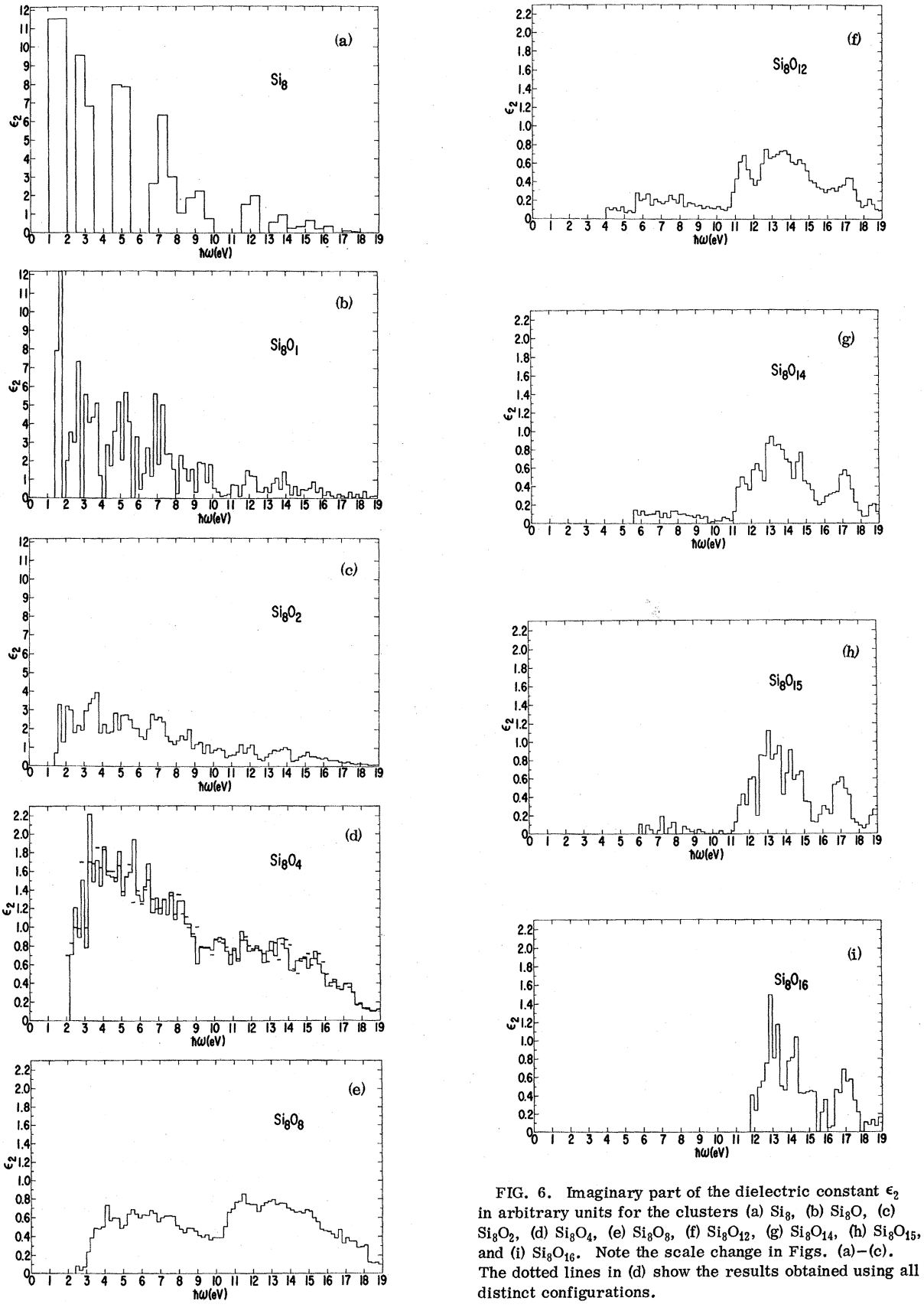

FIG. 6. Imaginary part of the dielectric constant ϵ_2 in arbitrary units for the clusters (a) Si_8, (b) Si_8O, (c) Si_8O_2, (d) Si_8O_4, (e) Si_8O_8, (f) Si_8O_{12}, (g) Si_8O_{14}, (h) Si_8O_{15}, and (i) Si_8O_{16}. Note the scale change in Figs. (a)–(c). The dotted lines in (d) show the results obtained using all distinct configurations.

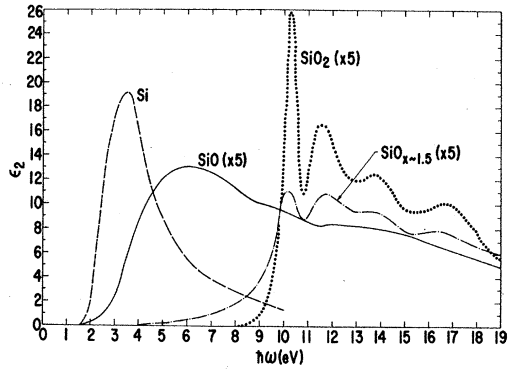

FIG. 7. Measured imaginary part of the dielectric constant ϵ_2 according to Philipp: dashed line, Si; solid line, SiO; dash-dot line, $SiO_{\sim 1.5}$; dotted line, SiO_2. Note change of scale for Si.

5. We note that these results for the energy gap differ a little from those obtained from the electronic density of states. The reason is that the present result for the energy gap is the smallest level difference between valence and conduction band states in any given cluster in our ensemble, while the energy gap from the average density of states gives the difference in energy between the lowest conduction-band state and the highest valence-band state in the entire ensemble. The latter is understandably smaller. We can argue that the present method is a more valid one of obtaining the gap and ϵ_2, but the difference is not very great, and either result appears to give good agreement with the experimental values. At any rate, the differences are probably less than the uncertainty brought about by the use of a finite cluster etc.

IV. CONCLUSIONS

Our treatment of the SiO_x system is clearly inadequate in many respects. The extended Hückel theory itself is crude, and, without any provision for charge consistency, is known to overestimate the ionicity. We expect in fact that the wave functions are not terribly good, which incidentally is a good reason for using the indirect-constant-matrix-element approximation. We have used an oversimplified model of the Si-O-Si bridges; it is known that the angle is usually somewhat different from 180°. We have not made our material really amorphous as we have maintained the topology of the diamond and/or β-crystobolite lattice. We have also omitted a consideration of defects, such as nonbridging oxygens and dangling Si bonds.

A further omission which is probably quite important is the matter of exciton absorption which in many insulators dominates the fundamental absorption edge. We expect that such an exciton would consist of a hole rather well localized on an oxygen and an electron mainly occupying the neighboring silicons. It is conceivable that the first large peak in the absorption edge, which is in fact lower in energy than our theoretical fundamental edge, corresponds to an exciton state. The possibility is certainly worth further investigation.

In spite of the above inadequacies, the fact that the results account for the main features of the optical absorption of compounds intermediate between Si and SiO_2 suggests that we have included the fundamental physics of the system in our treatment. Our results lend added weight to Philipp's model of a random network for this system.

In future work we hope to deepen our understanding of the electronic states of these systems by analytic treatments as well as to extend the cluster calculations.

ACKNOWLEDGMENT

We wish to thank Dr. H. Philipp for many helpful discussions and the use of his data before publication.

[1]See, e.g., D. Beaglehole and M. Zavetova, J. Non-Cryst. Solids 4, 272 (1970).

[2]See, e. g., A. P. Bradford and G. Hass, J. Opt. Soc. Am. 53, 1096 (1963); E. Ritter, Opt. Acta 9, 197 (1962).

[3]See, e. g., H. Philipp, Solid State Commun. 4, 73 (1966).

[4]H. Philipp, J. Phys. Chem. Solids (to be published).

[5]R. Grigorovici, J. Non-Cryst. Solids 1, 303 (1969).

[6]B. E. Warren, J. Appl. Phys. 8, 645 (1937); and R. C. Mozzi and B. E. Warren, J. Appl. Cryst. 2, 164 (1969).

[7]G. W. Brady, J. Phys. Chem. 63, 1119 (1959); S. C. H. Lin and M. Joshi, J. Electrochem. Soc. 116, 1740 (1969).

[8]L. Riechert and K. L. Weiner (unpublished); L. M. Roth (unpublished).

[9]B. Velicky, S. Kirkpatrick, and H. Ehrenreich, Phys. Rev. 175, 747 (1968).

[10]F. Bassani and D. Brust, Phys. Rev. 131, 1524 (1963).

[11]J. L. Beeby and S. F. Edwards, Proc. Roy. Soc. (London) A274, 395 (1963).

[12]P. Soven, Phys. Rev. 156, 809 (1967).

[13]P. Soven, Phys. Rev. 178, 1136 (1969).

[14]A. I. Gubanov, Dokl. Akad. Nauk 159, 46 (1964) [Sov. Phys. Doklady 9, 966 (1965)]; Fiz. Tverd. Tela. 7, 3145 (1965) [Sov. Phys. Solid State 7, 2547 (1966)].

[15]W. H. Butler and W. Kohn, J. Res. Natl. Bur. Std. (U.S.) 74A, 443 (1970).

[16]M. H. Brodsky and P. J. Stiles, Phys. Rev. Letters 25, 798 (1970).

[17]A. F. Ioffe and A. R. Regel, in *Progress in Semiconductors*, Vol. 4, edited by A. F. Gibson (Wiley, New York, 1960), p. 237.

[18]I. V. Abarenkov, A. V. Amosov, V. F. Bratsev,

and D. M. Yuden, Phys. Status Solidi 2, 865 (1970).
[19]A. J. Bennett, B. McCarroll, and R. P. Messmer, Surface Sci. 24, 191 (1971).
[20]A. J. Bennett, B. McCarroll, and R. P. Messmer, Phys. Rev. B 3, 1397 (1971).
[21]A. J. Bennett and L. M. Roth, J. Phys. Chem. Solids 32, 1251 (1971); L. M. Roth and A. J. Bennett, in *Proceedings of the Tenth International Conference on the Physics of Semiconductors, Cambridge, Mass.*, 1970 (U.S. AEC, Oak Ridge, 1970), p. 619.
[22]R. P. Messmer and G. D. Watkins, Phys. Rev. Letters 25, 656 (1970).
[23]R. W. G. Wyckoff, *Crystal Structures*, Vol. 1 (Interscience, N. Y., 1963).
[24]J. Stuke, J. Non-Cryst. Solids 4, 1 (1970).
[25]M. H. Brodsky and R. S. Title, Phys. Rev. Letters 23, 581 (1969).
[26]R. Hoffman, J. Chem. Phys. 36, 2179 (1962); 36, 2189 (1962); 40, 2474 (1963).
[27]K. Jug, Theoret. Chim. Acta (Berlin) 14, 91 (1969).
[28]T. M. Donovan and W. E. Spicer, Phys. Rev. Letters 21, 1572 (1968).
[29]T. L. Gilbert, in *Sigma Molecular Orbital Theory*, edited by O. Sinanoglŭ and K. B. Wiberg (Benjamin, New York, 1969), p. 249.
[30]L. C. Allen, in Ref. 29, p. 227.
[31]F. Herman and S. Skillman, *Atomic Structure Calculations* (Prentice-Hall, Englewood Cliffs, N. J., 1963).
[32]C. E. Moore, Natl. Bur. Std. (U. S.) Arch. No. 467 (1949) (unpublished).
[33]D. P. Santry and G. A. Segal, J. Chem. Phys. 47, 158 (1967); J. A. Pople and G. A. Segal, *ibid.* 43, 5136 (1965).
[34]D. W. J. Cruickshank, J. Chem. Soc. 5486 (1961).
[35]F. Bassani and M. Yoshimine, Phys. Rev. 130, 20 (1963).
[36]See, e.g., M. L. Cohen and T. K. Bergstresser, Phys. Rev. 141, 789 (1966), and references therein.
[37]R. P. Messmer (unpublished).
[38]R. C. Chaney, C. C. Lin, and E. E. Lafon, Phys. Rev. B 3, 459 (1971).

PHYSICAL REVIEW B VOLUME 4, NUMBER 8 15 OCTOBER 1971

Effect of Pressure on the Static Dielectric Constant of $KTaO_3$ †

W. R. Abel
Sandia Laboratories, Albuquerque, New Mexico 87115
(Received 27 May 1971)

The static dielectric constant ϵ of $KTaO_3$ has been measured from 4 to 300 K and at pressures up to 26 kbar. The temperature T_1 at which ϵ deviates from a Curie-Weiss law, attributed to quantum effects, is found to increase with increasing pressure with a slope $d\ln T_1/dP = 3\%/\text{kbar}$. At zero pressure, T_1 is 53 K. The pressure dependences of the Curie constant and Curie temperature were obtained also. The Curie constant decreases at the rate of 0.9%/kbar, and the Curie temperature decreases at the rate of 4.8 K/kbar. The reason for the increase of T_1 with pressure is discussed.

INTRODUCTION

It has long been known that ferroelectrics with very low Curie temperatures show deviations from the Curie-Weiss law for their dielectric response at temperatures much greater than the Curie temperature.[1,2] As the temperature of a paraelectric sample is lowered, a temperature (defined as T_1) is reached below which the static dielectric constant ϵ changes less rapidly than predicted by $\epsilon = B/(T - T_0)$. At temperatures much less than T_1, ϵ becomes temperature independent. A more precise definition of T_1 will be used later, but it is, in effect, the temperature at which the Curie-Weiss law fails. $SrTiO_3$ and $KTaO_3$ are examples of materials which exhibit this behavior. They both have a T_0 below 35 K, and start deviating from the Curie-Weiss law at a temperature of about 50 K. This behavior is usually attributed to quantum effects. Slater treated an ion in an anharmonic potential well classically in order to derive the ionic polarizability of a ferroelectric crystal in its paraelectric phase.[3] In 1952, J. H. Barrett[4] extended this theory by carrying out a quantum-mechanical treatment of the ionic polarizability. In his theory, the lowest quantum level for the ion has an energy equal to kT_1, so that for temperatures less than T_1 all ions are in their lowest energy states and further reduction in the temperature causes no change in the dielectric response. Barrett derived the relation

$$\epsilon = B/[\tfrac{1}{2} T_1 \coth(T_1/2T) - T_0] \ , \qquad (1)$$

and this seems to fit experiments quite well, if T_1, T_0, and B are treated as empirically determined constants. Barrett was not successful in determining these constants from first principles.

Pressure experiments have been made on many ferroelectrics in order to find the volume dependence of T_0 and the Curie constant B, effects which are now fairly well understood.[5] However, apparently no study of the volume dependence of T_1